

# Noise characteristics of twin-square slot jets

**V. Boopathi Sabareesh, K. Srinivasan\* and T. Sundararajan**

*Department of Mechanical Engineering Indian Institute of Technology Madras  
Chennai - 600036, India*

Acoustic measurements have been undertaken on two different twin square jet topologies. OASPL, spectra, directivity measurement and shock-cell visualization have been conducted to evaluate twin square jets in different edge-vertex orientations. The results indicate that twin square jets effectively suppress noise up to 4 dB in terms of OASPL and 6 dB in terms of screech tonal SPL compared to an equivalent single circular jet. The study promises that twin-jet topology could serve as an effective tool for noise suppression.

## 1. INTRODUCTION

The twin jet arrangement is employed in various disciplines such as aerospace, automotive, and agricultural engineering. Some specific engineering applications include spraying, cleaning and cooling. In several such applications, noise emission is as much a concern as the hydrodynamic performance. In many jet flow applications, objectives encompass both mixing enhancement and noise suppression. Mixing enhancement is achieved by encouraging the interactions between small and large scale flow structures. Non-circular jets accomplish this by promoting both streamwise and spanwise vorticity. The interplay of these features leads to interesting phenomena such as axis switching in such jets [1-5]. Twin non-circular jets exhibit further complexity due to the interaction between the two jets.

Jet noise is essentially composed of turbulent mixing noise [6] and shock associated noise. Shock associated noise is further classified into screech [7] and broadband shock associated noise [8]. Shock associated noise is generated due to imperfect jet expansion at the nozzle exit causing a series of shock cells in the flow field. When two jets are placed in close vicinity, coupling between the jet plumes can occur leading to amplification of screech tones and enhanced dynamic pressures in the inter-nozzle region [9-13]. This could cause structural fatigue damage to the nozzle and surrounding parts. Plenty of literature exists on twin jets, e.g., [9-13], and therefore, only a sample of the relevant literature is discussed below.

Seiner et al. [9] reported that the higher dynamic pressures in the inter nozzle region are associated with the phase coupling of each plume's jet flapping mode. Their investigation on various suppression methods revealed that small tabs mounted on the nozzle exit provided substantial noise reduction compared to small notches at the exit. Wlezien and coworkers conducted numerous investigations on the coupling of high speed twin jets from regular/asymmetric geometries. For instance, Wlezien [10] examined the coupling between twin convergent nozzles and found that coupling occurs at lower spacings at lower Mach numbers and at higher Mach numbers at higher spacings. Shaw [11] explored the effectiveness of various noise suppression techniques. It was concluded that except axial spacing, all other techniques such as tabs, lateral spacing and secondary jet are very effective in the suppression of noise. Raman

\*Corresponding author. Email: ksri@iitm.ac.in

and Taghavi [12] provided the correlation parameter to determine the mode of coupling in rectangular twin jet. Raman [13] documented the coupling of the screech instabilities in twin jets of complex geometry.

Bhat [14] investigated the acoustic characteristics of two parallel flow circular jets for both similar and dissimilar flow cases with equal and unequal tubes. It was found that the noise from two parallel jets with similar and dissimilar flow is quieter than the equivalent single jet in the plane containing the two axes.

Clauss *et al.* [15] tested the over/under wing engine arrangement for a supersonic cruise vehicle (SCV). The noise reduction was attributed to the acoustic shielding of the upper jet by the lower jet. Further Parthasarathy *et al.* [16] developed an analytical model for the twin jet shielding analysis to quantify the perceived noise levels and noise reduction of the over/under wing engine arrangement.

Kantola [17] performed experiments on heated twin jets in both circular and non circular configurations to evaluate out the effect of turbulent mixing and acoustic shielding on jet noise by varying the spacing between the two jets. Most of the noise reduction was obtained for a large jet spacing since the inter nozzle shielding layer covers the large part of the jet downstream. Further, the noise generated from the twin jet was lower than the sum of acoustic energy from the two independent jets.

Shivasankara and Bhat [18] demonstrated noise reduction in a high velocity jet by placing a second jet of lower velocity. The observed noise reduction was due to acoustic shielding since there is no significant mean flow interaction between the two jets up to 5 diameters downstream of the nozzle exit. The peak noise reduction was found along the plane containing the two jet axes and along the side where the lower velocity jet is located between the high velocity jet and the observer.

Srinivasan *et al.* [19] performed experiments on twin elliptic jets and showed the importance of aspect ratio of the twin jet on the noise reduction. Panicker *et al.* [20] studied coupled twin jets of single beveled geometry for both arrowhead and V shaped configurations. They found that the coupling occurred in V shaped configuration but not in the arrowhead configuration.

Morris *et al.* [21] reported that the alteration of angle between the two jets results in peak noise reduction and change in the jet noise directivity pattern. The cause for this noise reduction was noticed as a function of velocity and temperature difference between the two jets. Gerhold [22] developed a two dimensional analytical model to investigate the phenomenon of acoustic shielding. The shielding of a point source near the cylindrical jet was also modeled to derive the directivity function [23]. Yu and Fretallo [24] examined the acoustic shielding by a turbulent jet. It was observed that the noise reduction due to acoustic shielding depends upon the balance between the refraction and diffraction. Lancey [25] formulated a three dimensional quadrupole source model by applying the reciprocal theorem to the known monopole source model [23].

## 1.1. OBJECTIVES OF THE PRESENT WORK

Although the characteristics of single non-circular jets abound the literature, information about twin-non-circular orifice jets is scarce. Therefore, the present study focuses on the behavior of twin non-circular slot jets to explore the effect of the twin-jet configuration on the noise emission. Twin-square-jets are studied in two possible configurations: edge aligned with edge, and vertex aligned with vertex. The schematic of the geometries under considered and the nomenclature is shown in Fig. 1. The twin-jet noise is compared against the baseline case of a single circular

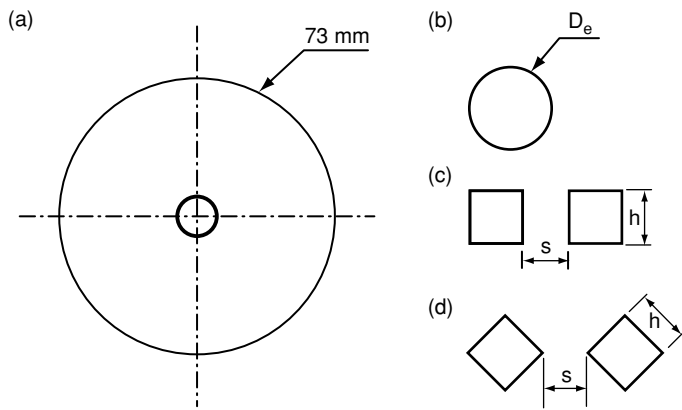


Figure 1: Disk Nozzle configuration; (a) Disk nozzle (b) Equivalent Single jet (c) Edge faced twin jet (d) Vertex faced twin jet.

slot jet of the same area. This assumption is reasonable since the boundary layer growth inside slot jets is negligible, resulting in the same total momentum.

## 2. EXPERIMENTAL SET UP AND PROCEDURE

### 2.1. TEST FACILITY

Figure 2 shows the schematic view of the experimental set up. All the experiments were conducted within a simple anechoic chamber of dimensions  $2.5 \text{ m} \times 2 \text{ m} \times 2 \text{ m}$ . The inner walls of anechoic chamber are completely covered with polyurethane foam to make a free field environment inside the chamber. The lower cut off frequency of the chamber is 630 Hz. The settling chamber having an inner diameter of 380 mm and the traversing system for the directivity measurement are placed inside the anechoic chamber. Acoustic foam is pasted on all the reflective surfaces of the settling chamber and traversing system to avoid internal reflections. The inner wall of the settling chamber is also lined with acoustic foam to reduce the structure-borne acoustic disturbances. Flow conditioning meshes of progressive fineness is kept inside the settling chamber to reduce the initial turbulence level. The disk

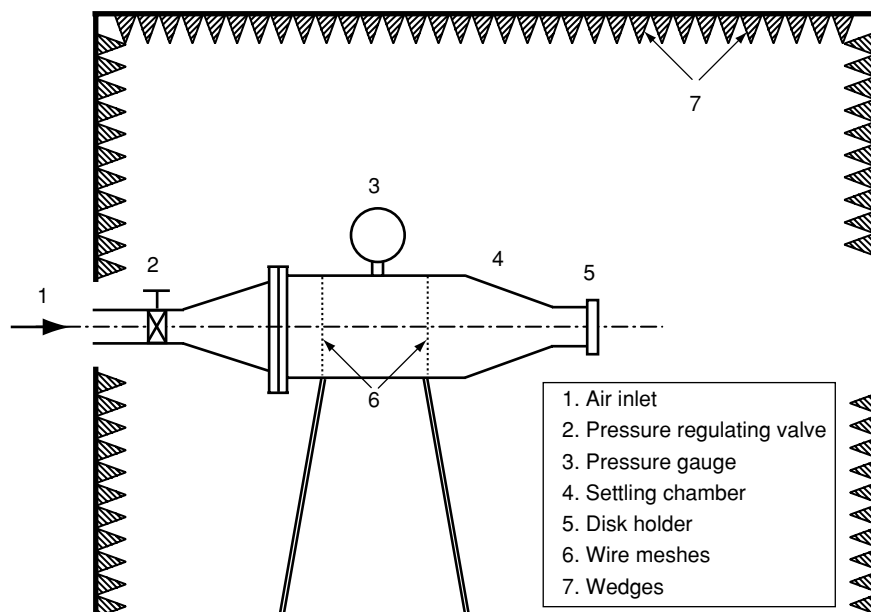


Figure 2: Schematic view of anechoic chamber.

nozzle is attached to the converged end section of the settling chamber having a diameter of 43.5 mm by the use of a disk holder. To control the stagnation pressure of the settling chamber, a needle valve was used. The settling chamber was supplied with compressed air at pressures up to 7 bar from two tanks of capacity 10 m<sup>3</sup> each. A two stage reciprocating air compressor of 150 hp capacity is used to pressurize the air.

## 2.2. DISK NOZZLE CONFIGURATION

The schematic views of the slot or disk nozzle configuration used in this experiment are shown in Fig. 1. The twin jet disk nozzles were fabricated for the different configurations and various jet spacing ( $s/h = 0.5$  to 2) using a circular mild steel plate of diameter 73 mm and 2 mm thickness. The twin slot jets are designed for constant area equivalent to that of the circular single jet of diameter 10 mm. The edge-edge aligned configuration is henceforth referred as Ed-Ed configuration and the vertex-vertex aligned case as Vx-Vx configuration.

## 2.3. INSTRUMENTATION

The measurements include shadowgraph images and acoustic pressure data. The shadowgraph apparatus comprised a high resolution (1280 × 1024 pixel - Mikrotron Model No. 1302 CMOS Type) digital video camera, high intensity light source, bi-convex lens (75 mm diameter), and a computer. An optical fiber cable links the camera to the computer, in which the results are viewed/stored. A quarter inch condenser microphone (PCB Piezotronics, Model No. 377A01), with an open circuit sensitivity of 4 mV/Pa at 250 Hz is used for the acoustic measurements. The microphone is calibrated using a pistonphone calibrator. The microphone is attached to the rotating arm of the automatic angular traversing system in which a stepper motor is employed to achieve the required angular movement for the directivity measurement. The arrangement of this traverse mechanism is shown in Fig.3. For the single jet measurement, the rotating arm with microphone is kept such that whenever the arm is rotated then the microphone always faces the jet exit center and aligned with the jet axis. In the case of twin jets, the measurement plane passes through the geometric centre of the twin jet configuration. The stepper motor is driven by a stepper drive (National Instruments NI-MID-7604). Measurements in the azimuthal direction are carried out by simply rotating the model with respect to the reference point. The traversing system is synchronized with the data acquisition system. The signal is low pass filtered at 70 KHz using

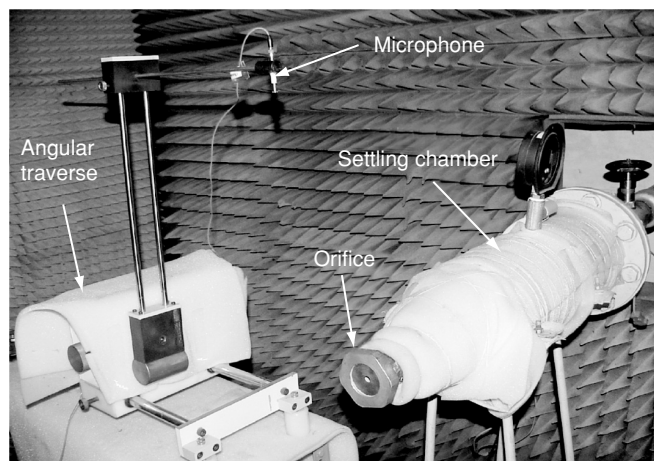


Figure 3: Photograph showing the arrangement of traverse mechanism.

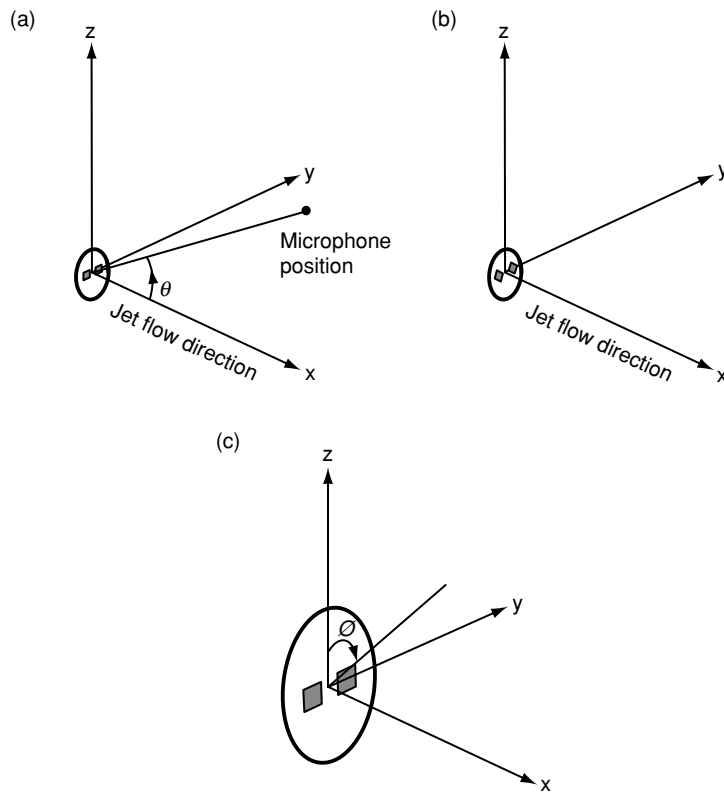


Figure 4: Coordinate system and directivity measurement conventions used.  $q$  is measured from downstream jet axis for various  $\phi$ . (a) twin jet (Ed-Ed); (b) twin Jet (Vx-Vx), (c) Azimuthal angle ( $\phi$ ) convention.

analog filter (Krohn-Hite Model No. 3364), and is sampled at the rate of 150 Sa/s. The signal is acquired for a time period of one second through an eight channel simultaneous sampling card (National Instruments, Model No. NI-PCI-6143). Both data acquisition and traverse motion is automated and controlled using LABVIEW software 7.1.

The far field measurement is made at  $40 De$  from the jet axis. The directivity measurement along the jet axis is obtained by moving the microphone from  $27^\circ \leq \theta \leq 145^\circ$ . The directivity measurement in the azimuthal direction is obtained by rotating the model from  $0^\circ \leq \phi \leq 90^\circ$  as shown in Fig. 4.

## 2.4. UNCERTAINTY ESTIMATES

The equivalent diameter of the twin jet model is within  $10 \pm 0.02$  mm. The reported sound pressure levels are repeatable within  $\pm 1$  dB, and the reference pressure is  $20 \mu\text{Pa}$ . The uncertainty estimate for the stagnation pressure of the settling chamber is  $\pm 2\%$  of the full scale and for the temperature inside the anechoic chamber is  $\pm 1^\circ\text{C}$ . The frequency resolution based on the FFT size is 37 Hz.

## 3. RESULTS AND DISCUSSION

The results have been organized to bring out the effect of spacing leading to variations in interactions between the jets, effect of nozzle pressure ratio, sound pressure directivity, and shielding mechanisms in twin jets. These are presented in the following subsections.

### 3.1. EFFECT OF SPACING

The SPL spectra for single jets (circular and square geometries) and twin jet

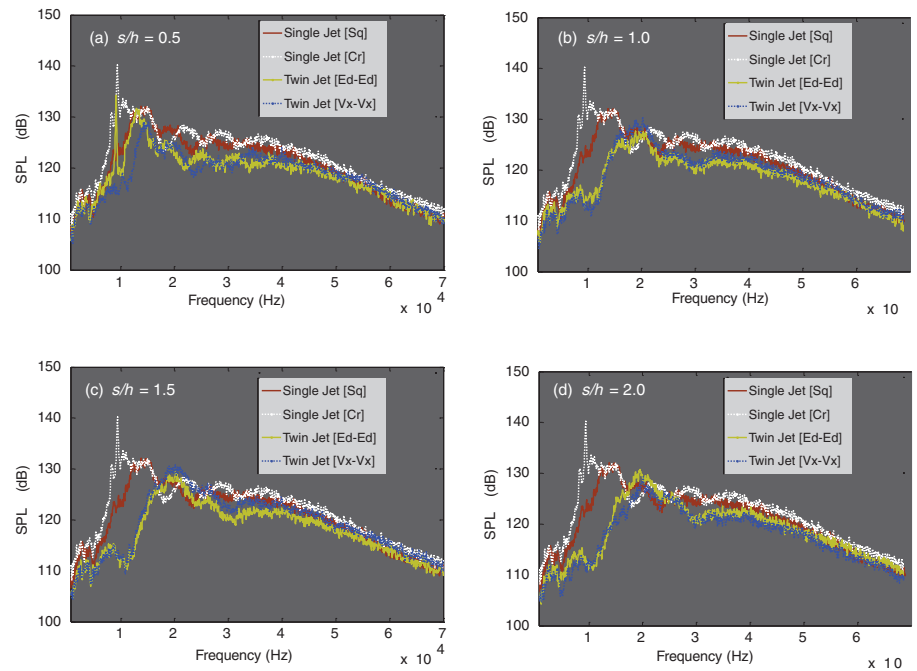


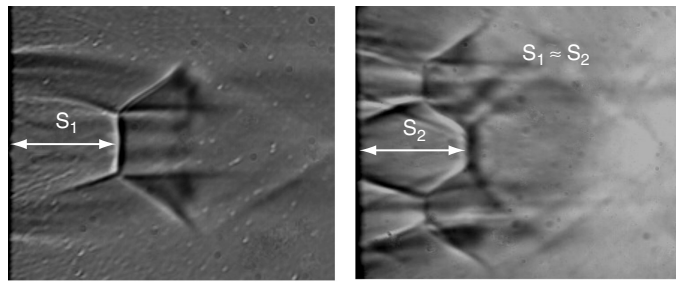
Figure 5: Spectra from single and twin jets at NPR = 7 for various jet spacing.

configurations for various spacings are shown in Fig. 5 for NPR = 7. The screech tones are observed around 10 kHz from the circular jet and edge faced twin jet (Twin Jet: Ed-Ed) configuration for a jet spacing  $s/h = 0.5$ . A small variation in the shock cell length between the circular jet and twin square jet (Twin Jet: Ed-Ed) as shown in Fig. 6(a), leads to a corresponding difference in the screech tone frequency of 220 Hz. Screech tone is found to be absent for the vertex faced twin jet (Twin Jet: Vx-Vx) configuration at  $s/h = 0.5$  and single square jet. The screech tone amplitude of the circular jet is 6 dB higher than that of the twin square jet configuration (Twin Jet: Ed-Ed). When  $s/h$  is increased from 0.5 to 2, there is no screech found in both the twin jet configurations. Only at  $s/h = 0.5$ , the edge faced twin jet (Twin Jet: Ed-Ed) generates screech tone due to the strong normal shock produced by the interaction of the two jets. The twin jet interaction in the Ed-Ed configuration at  $s/h = 0.5$  is clearly observed from the shadowgraph image [Fig. 6(b)]. It is observed from Fig. 6 that there is no distortion in the shock cell system of the two jet plumes in Vx-Vx configuration, whereas Ed-Ed configuration displays a crucial shock cell distortion due to the jet interaction at  $s/h = 0.5$ . Since there is no jet interaction at  $s/h > 0.5$  for the both twin jet configurations, the twin jet spectra in Fig. 5 does not show discrete screech tones.

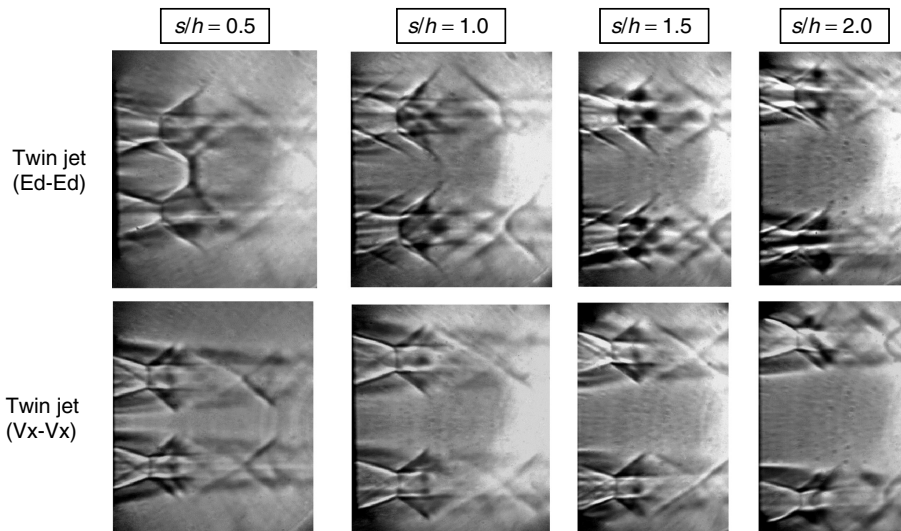
The shadowgraph image [Fig. 6(b)] shows even though the jet spacing is same ( $s/h = 0.5$ ) for both Ed-Ed and Vx-Vx configuration, interaction between the jets takes place only in the Ed-Ed configuration. This may be due to the jet plume rotation reported by Quinn [3] leading to further proximity of the two jet plumes in the Ed-Ed configuration. By a similar argument, the jet plume rotation in Vx-Vx jets would widen the spacing between the jets more than before, thereby inhibiting the interaction between the jets.

### 3.2. EFFECT OF NPR

The shadowgraph images with spectra at various NPR from 7 to 5.5 are shown in Fig. 7 for Ed-Ed twin jet configuration. As pointed out earlier, in Fig. 6, the individual



(a) Shock-cell length comparison for circular jet and twin square jet (Ed-Ed)



(b) Twin jets for various jet spacings

Figure 6: Shadowgraph images of circular jet and twin square jets at  $NPR = 7$ .

shock-cells in Ed-Ed configuration interact and coalesce to form a strong normal shock at certain pressure ratios. Figure 7 reveals that inter-jet interaction is absent at lower pressure ratios and sets in at an NPR value of 6. Consequently, screech tones due to twin-jet interactions vanish at lower values of NPR. However, as it will be shown in a later section, screech resurfaces at lower values of NPR around 3 or 4, due to individual jet mechanisms. The interactions are only set up at  $NPR \geq 6$  and vanish at lower NPR. At lower NPR around 3 or 4, both jets are screeching individually but not interacting. The decrease in shock cell length with decrease in NPR, increases the screech tone frequency. Since there is no interaction between the two jets in the Vx-Vx configuration, there is no screech in these jets. The absence of shock-interactions and coalescence and the absence of screech in the corresponding acoustic spectra are clearly understood from Fig. 8.

A further decrease in NPR ( $< 5$ ) results in a low amplitude screech tone in both Ed-Ed (Fig. 9) and Vx-Vx twin jets (Fig. 10). This is due to the individual feedback loops present in the two component jets. The reduction in the fully expanded jet dimension with reduction in NPR leads to the possibility of individual screech feedback loops to operate in the two jets, thereby promoting screech. Thus, even in the absence of inter-jet interactions, screech tones can occur. The following are the differences between screech tones in interacting and non-interacting twin jets: (a) the screech amplitudes in interacting twin-jets are higher than those in the non-interacting case, (b) frequencies in the non-interacting jets are higher than those in the interacting jets, due to the smaller length scales involved, and (c) screech due to inter-jet interactions occur above NPR value of 5 whereas, the screech in non-interacting jets is observed below NPR value of 5. These phenomena are clearly

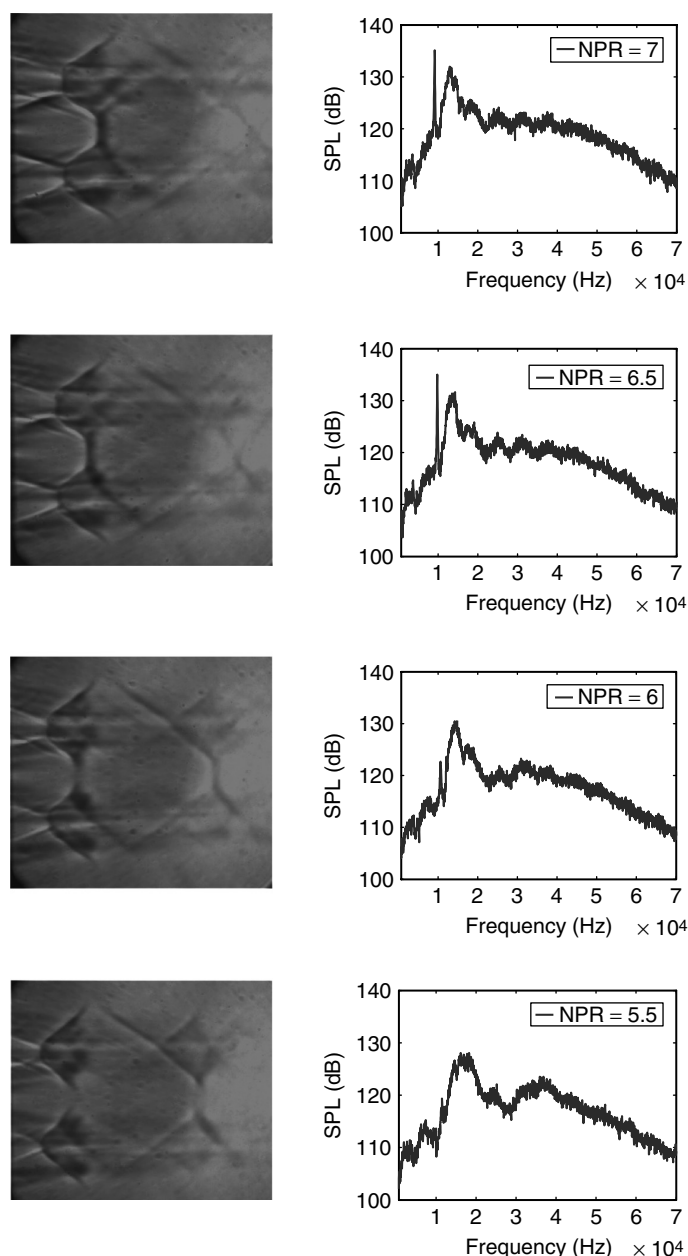


Figure 7: Shadowgraph images of Twin Jet (Ed-Ed) with spectra at NPR 7 to 5.5 at  $s/h = 0.5$ .

demarcated in the color maps of spectra shown in Figs. 11 and 12.

The color map in Fig. 11 shows the frequency versus NPR plot of Ed-Ed twin jet for  $s/h = 0.5$ . In this plot, the red lines represent the discrete screech tone. These screech tones are observed in two regions; one region in the NPR range of 3.5 to 4.5, and another between 5.5 and 7. However, in the case of Vx-Vx twin jet (Fig. 12), only one region is observed between NPR 3.5 and 4.5. This is due to the absence of jet interactions in Vx-Vx configuration. At higher spacings, jet interactions are absent for both Ed-Ed and Vx-Vx configurations, emphasizing the importance of inter-nozzle spacing on the spectral behavior.

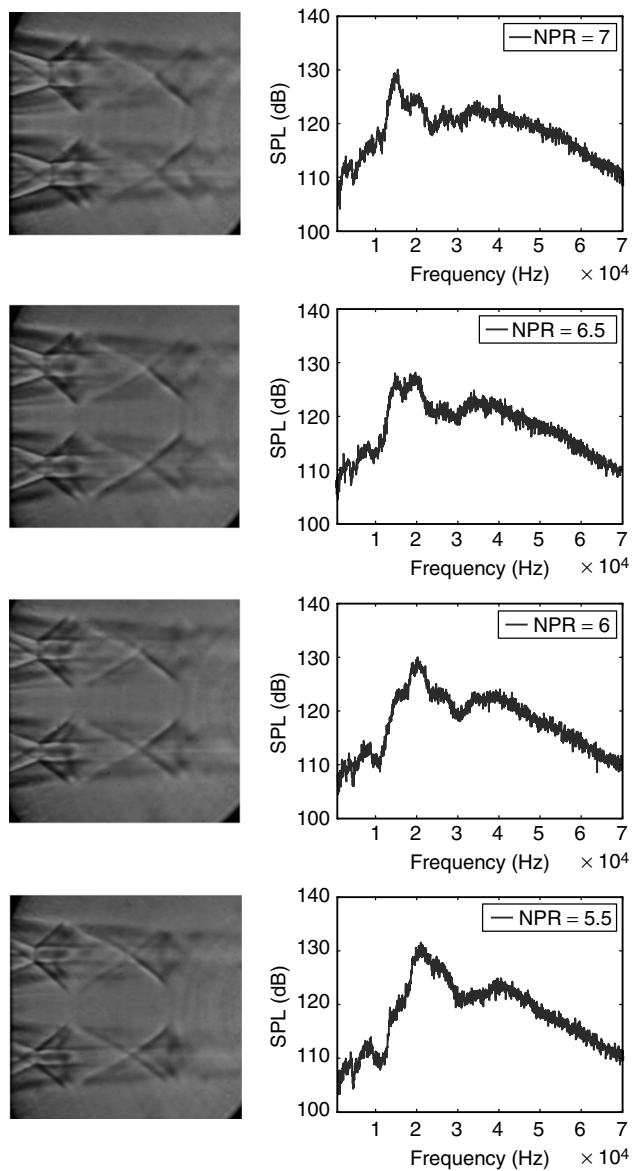


Figure 8: Shadowgraph images of Twin Jet (Vx-Vx) with spectra at NPR 7 to 5.5 at  $s/h = 0.5$ .

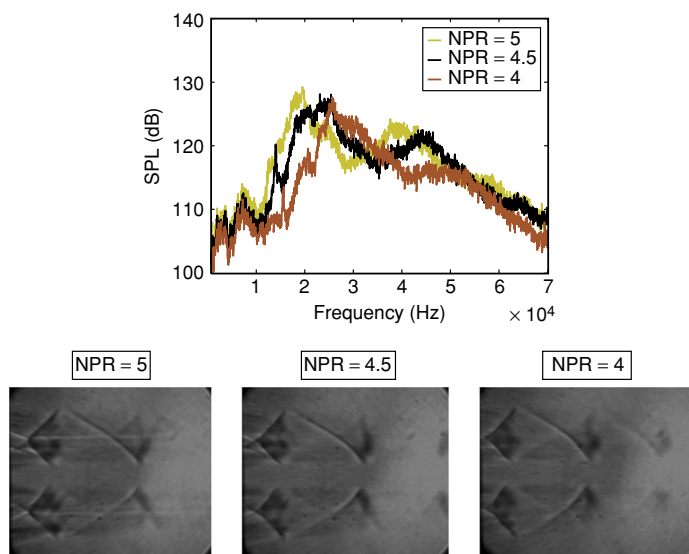


Figure 9: Shadowgraph images of Twin Jet (Ed-Ed) with spectra at NPR 5 to 4 at  $s/h = 0.5$ .

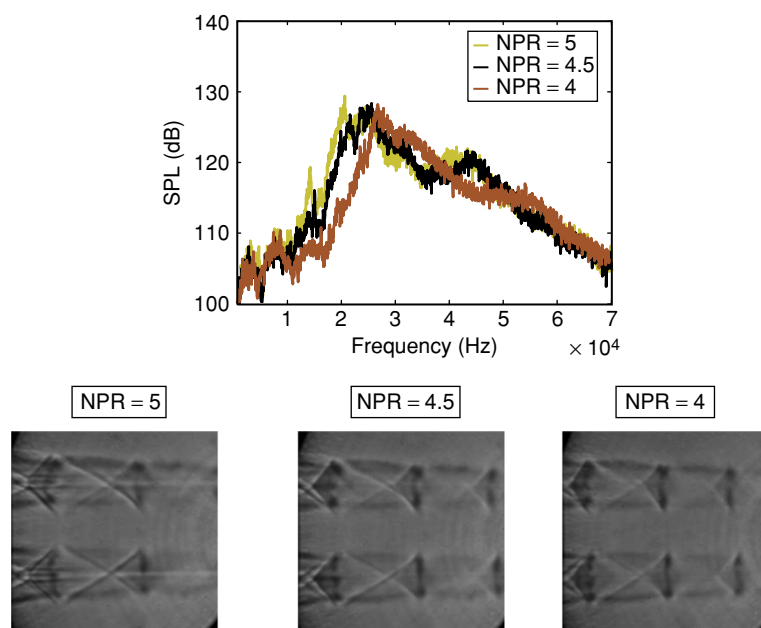


Figure 10: Shadowgraph images of Twin Jet ( $V_x$ - $V_x$ ) with spectra at NPR 5 to 4 at  $s/h = 0.5$ .

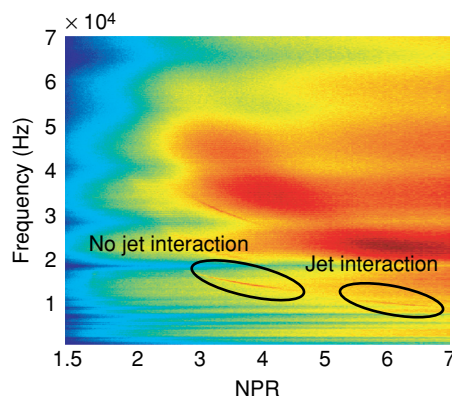


Figure 11: Color map shows the screech frequencies of Twin Jet ( $Ed$ - $Ed$ ) for  $s/h = 0.5$ .

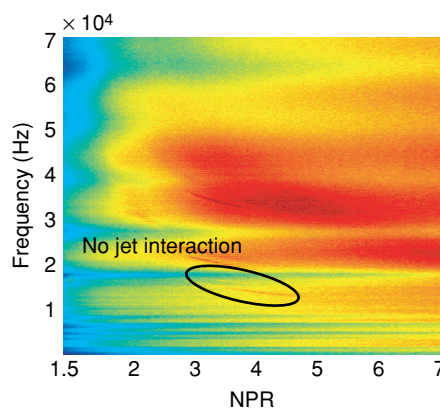


Figure 12: Color map shows the screech frequencies of Twin Jet ( $V_x$ - $V_x$ ) for  $s/h = 0.5$ .

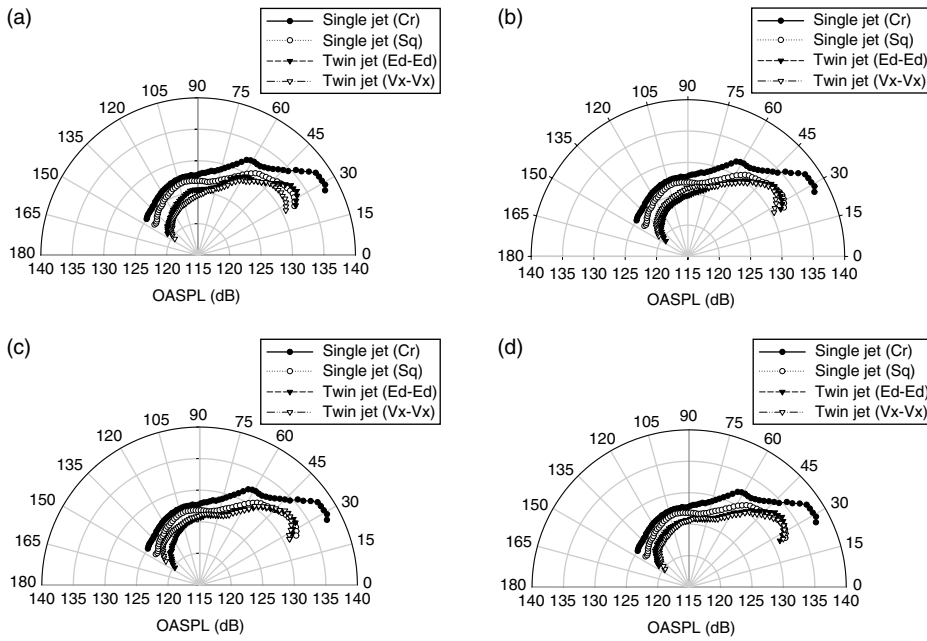


Figure 13: OASPL of single and twin jets for  $NPR = 7$ , (a)  $s/h = 0.5$ , (b)  $s/h = 1$ , (c)  $s/h = 1.5$  (d)  $s/h = 2.0$ .

### 3.3. OASPL AND DIRECTIVITY

The OASPLs of the single jet and twin jets of both Ed-Ed and Vx-Vx configurations are compared in Fig. 13 for various jet spacing. Both twin jets show a noise reduction of about 4 dB at all jet spacings, compared to single circular and square jets. In general, the twin jets have close values of OASPL, with Ed-Ed configuration being slightly noisier in the downstream direction. It is well known that non circular jets with sharp corners generate fine scale turbulence structures from the sharp corners leading to low intensity mixing noise. This is the reason for the reduction in OASPLs for the twin jets compared to the single jets.

Figure 14 shows the grayscale spectra for both the Ed-Ed and Vx-Vx twin jets at  $s/h = 0.5$ . The presence of screech tone throughout the angles  $27^\circ$  to  $145^\circ$  by the Ed-Ed configuration is seen in Fig. 14(a) as a thin white line and the absence of screech tone in the Vx-Vx twin jet is observed from Fig. 14(b).

The OASPL plots of twin jets (Ed-Ed and Vx-Vx) are shown in Fig. 15. It is clear from the figure that OASPL values are higher in the downstream angles. An increase in OASPL over the entire range of angles from  $27^\circ$  to  $145^\circ$  is seen in Fig. 15(a) for the Ed-Ed twin jet with increasing NPR. Both Ed-Ed and Vx-Vx twin jet show an increase in OASPL for angles less than  $80^\circ$  and the opposite trend for angles above  $80^\circ$  as shown in Fig. 15(b-h).

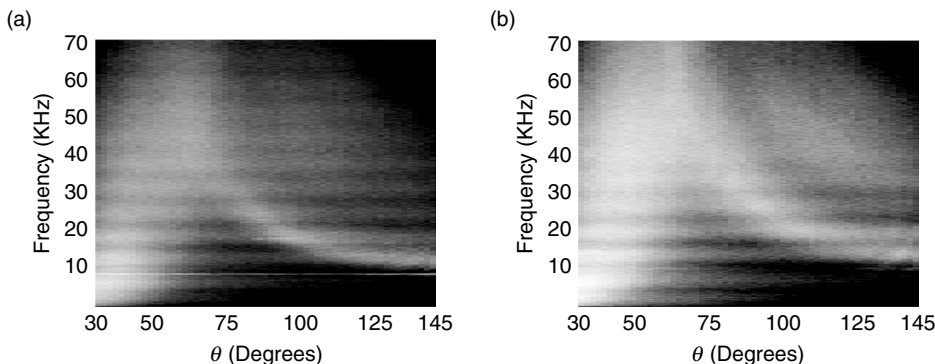


Figure 14: Grayscale Spectra for (a) Twin Jet (Ed-Ed) and (b) Twin Jet (Vx-Vx) for  $NPR = 7$ ,  $s/h = 0.5$ .

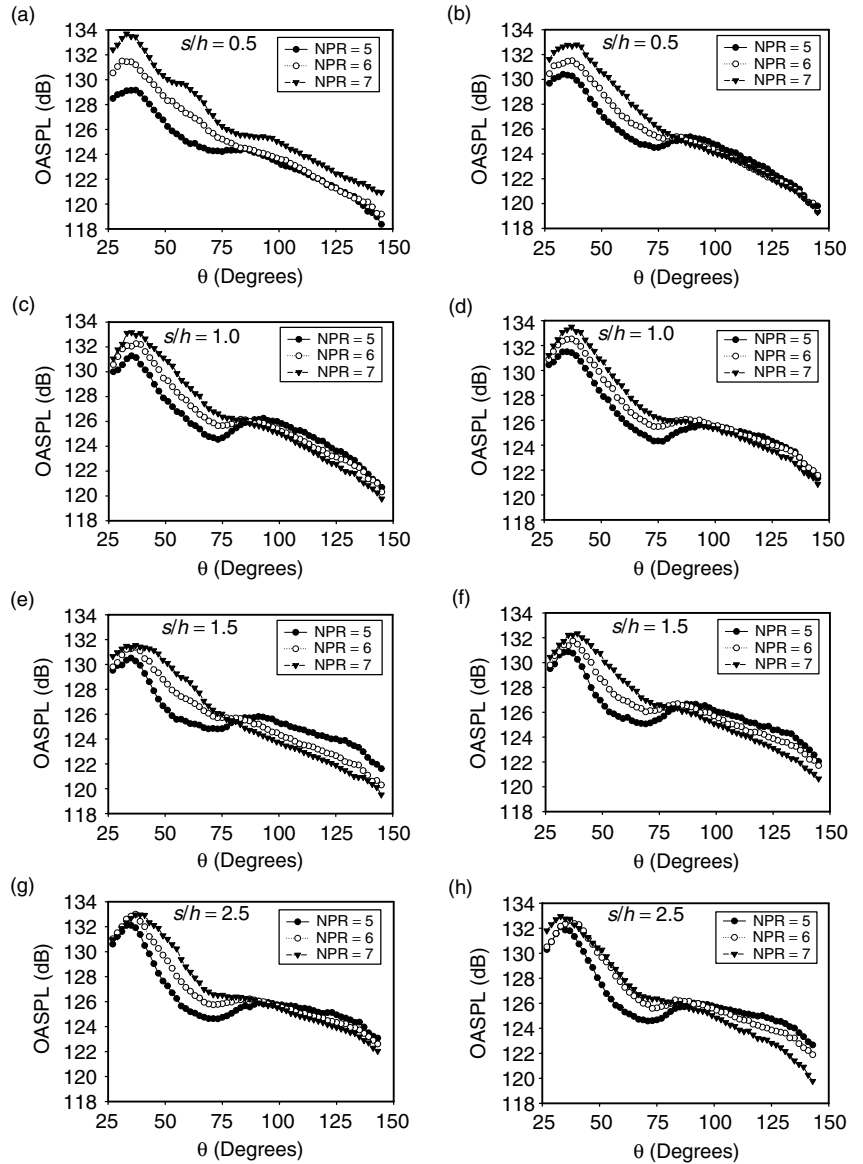


Figure 15: *OASPL plot of twin jet; (a-d) Twin Jet (Ed-Ed); (e-h) Twin Jet (Vx-Vx).*

The waterfall spectra of Ed-Ed and Vx-Vx twin jets at NPR values of 5 and 7 are compared at various emission angles in Fig. 16. In the case of Ed-Ed twin jet, noise amplitudes are higher at NPR value of 7 compared to those at 5. The variation is large within about 30 kHz, and levels off beyond that frequency. For the Ed-Ed twin jet, noise components such as screech and broadband shock associated noise are higher at NPR = 7. In both Ed-Ed and Vx-Vx jets, the predominance of BSAN leads to an accentuation of OASPL in the upstream angles ( $90^{\circ}$ – $145^{\circ}$ ). This trend is more pronounced at lower NPRs.

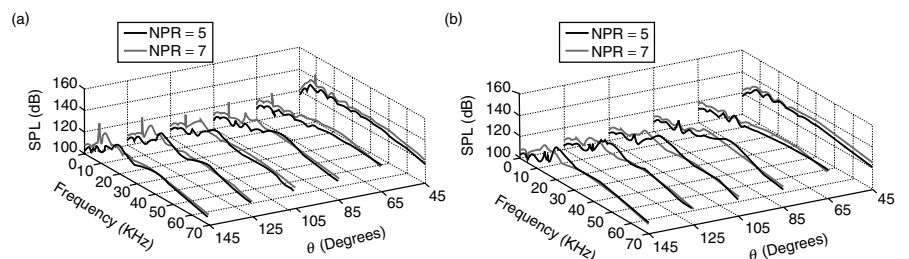


Figure 16: *Waterfall spectra of twin jet for NPR 5 & 7 at  $s/h = 0.5$ ; (a) Twin Jet (Ed-Ed) (b) Twin Jet (Vx-Vx).*

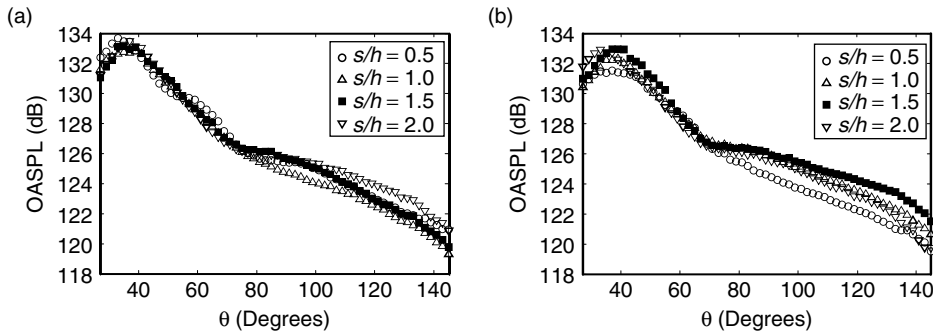


Figure 17: OASPL comparison for different jet spacing; (a) Twin Jet (Ed-Ed) (b) Twin Jet (Vx-Vx) for NPR = 7.

Figure 17 shows the effect of spacing on OASPL for the Ed-Ed and Vx-Vx twin jets. It is observed that the OASPLs lie within  $\pm 2$  dB of each other at all angles. These plots reveal the fact that while spacing can significantly affect the spectra by way of inter-jet interactions, there is little variation in the OASPL among the jets with various spacings. Thus, spacing is not an effective tool to reduce the overall noise. The sonic fatigue could be related to the unsteady pressure fluctuations produced by the screech tone generation in the inter nozzle region of interacting twin jet. So the sonic fatigue possibility could be averted by avoiding the screech tone generation in twin by increasing the jet spacing. However, the sonic fatigue possibility could be averted by avoiding small inter-jet spacings.

### 3.4. AZIMUTHAL VARIATION OF NOISE

Figures 18 and 19 present the OASPL comparison between single and twin jets measured at two different planes;  $\phi = 0^\circ$  and  $90^\circ$ , at NPR values of 3 and 7. At a lower value of NPR = 3, the noise benefits of twin jets are visible only at certain

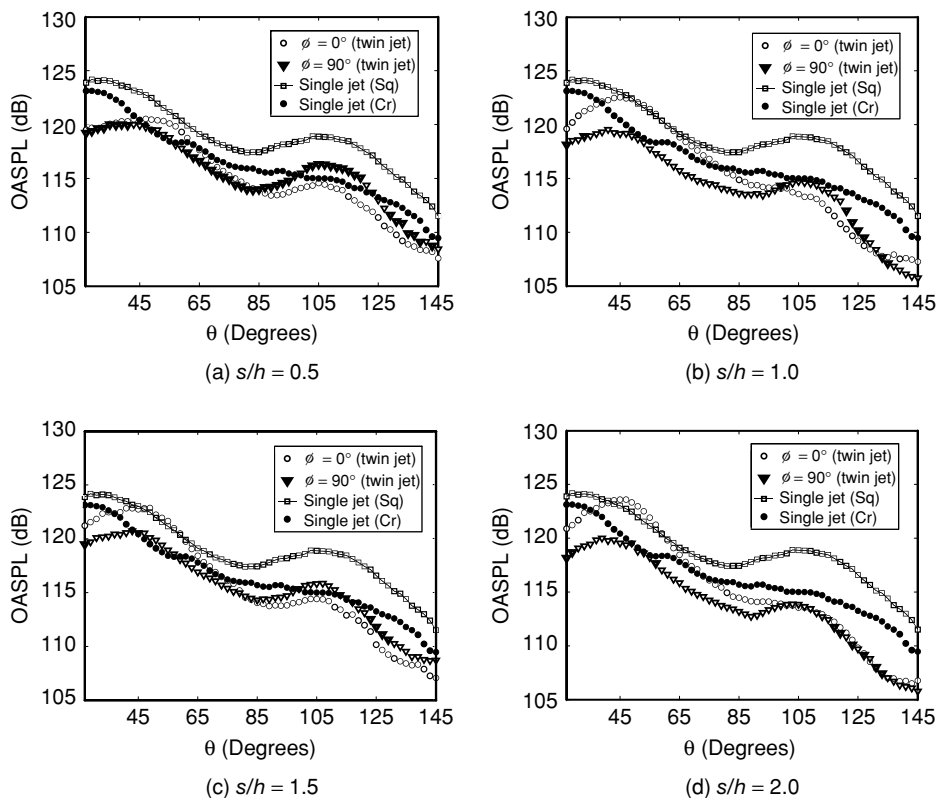


Figure 18: OASPL comparison of Twin Jet (Ed-Ed) with single jet at NPR = 3.

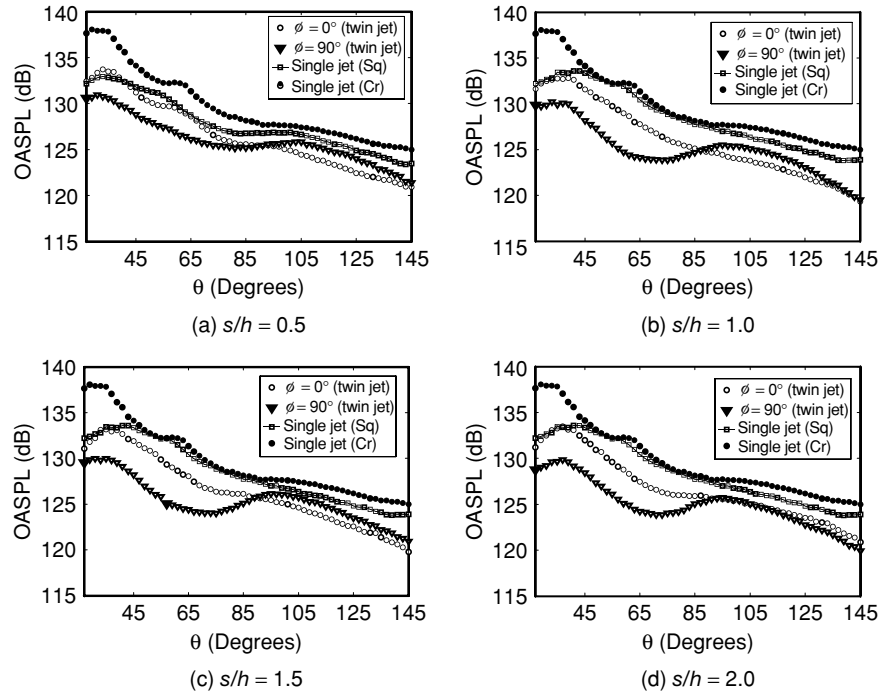


Figure 19: OASPL comparison of Twin Jet (Ed-Ed) with single jet at  $NPR = 7$ .

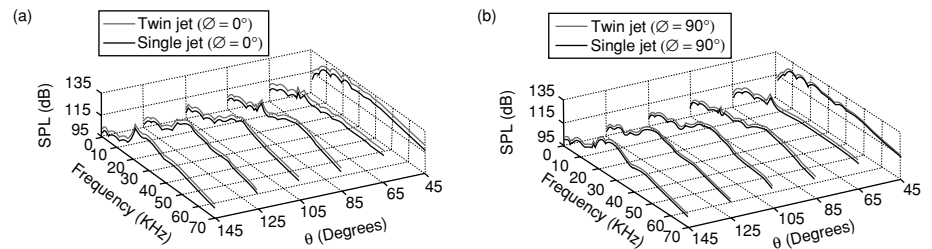


Figure 20: Waterfall spectra comparison of vertex faced twin jet with single jet at  $NPR = 4.5$  and  $s/h = 1.5$ ; (a)  $\phi = 0^\circ$  and (b)  $\phi = 90^\circ$ .

upstream observer angles. The trends are similar for Vx-Vx twin jet also. The reason for this behaviour is that the mixing enhancement brought forth by the twin jets enhances mixing noise at these conditions. However, at a higher NPR value of 7, the noise benefits of twin jets are evident. A noise reduction of 5 dB is at  $\phi = 90^\circ$ . In this case, noise benefits are higher in the downstream direction.

### 3.5. ACOUSTIC SHIELDING

The interaction of flow features and acoustic waves between the two jets in a twin jet configuration plays an immense role in the far-field acoustic behavior. These effects may lead to either amplification or attenuation of broad band jet noise. Therefore, the role of these effects on jet noise is analyzed to quantify the acoustic shielding effect in twin jets. The acoustic shielding effect is studied by carrying out measurements in twin jets and in single jets with one of the jets closed. The single jet measurement was carried out by blocking the flow path of one of two jets. Figure 20 shows the spectral comparison of twin jet with single jet at two different angles  $\phi = 0^\circ$  and  $\phi = 90^\circ$  at  $NPR 4.5$  for Vx-Vx twin jet.

The amplification in the broadband noise spectral components in the Vx-Vx twin jet over the range  $45^\circ \leq \theta \leq 145^\circ$  reveals the effect of a neighboring jet on noise at  $\phi = 0^\circ$ . However, this effect is absent at  $\phi = 90^\circ$  in the range  $45^\circ \leq \theta \leq 85^\circ$ . Further, OASPL comparison of twin jets with single jet presented in Fig. 21. Since

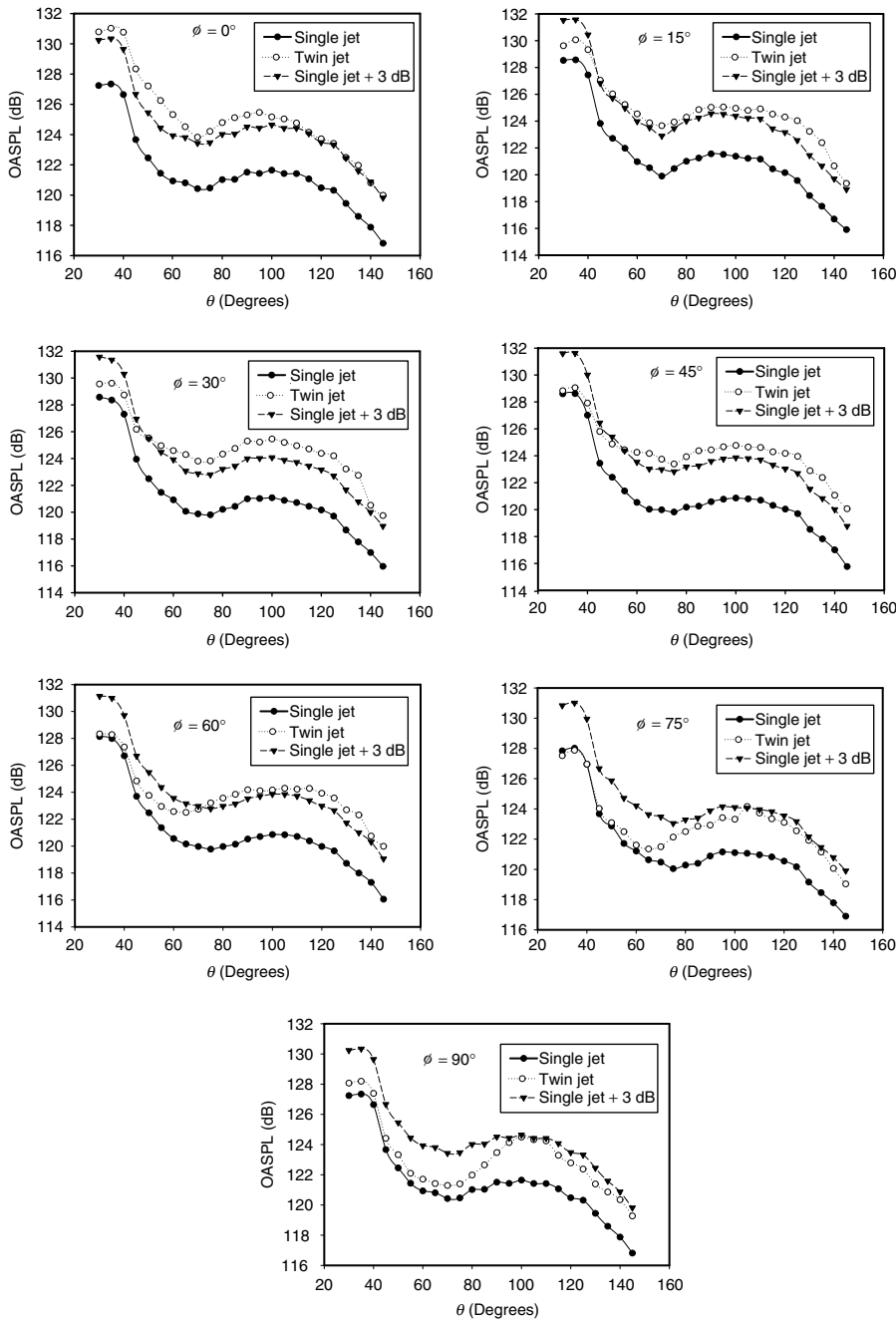


Figure 21: OASPL comparison of twin jet with single jet for vertex faced twin jet at  $NPR = 4.5$  and  $s/h = 1.5$  in the azimuthal direction.

the addition of two equal and identical uncorrelated noise sources would correspond to an increase of 3 dB, the twin jets are compared to single jet with addition of 3 dB. It is clear from this figure that as  $\phi$  varies from  $0^\circ$  to  $90^\circ$ , the twin jets become quieter than the theoretical value of 3 dB above single jet. This observation, is however valid only in the downstream angles of  $27^\circ \leq \theta \leq 90^\circ$ . This behaviour can be attributed to the dominance of flow features (jet plume rotation, streamwise vorticity growth, etc.) in the downstream direction.

The effect of acoustic shielding can be quantified by comparing the acoustic power values of single jet (one jet blocked) and the twin jet ( $V_x V_x$ ). The acoustic power radiated by the single jet is 1.099 W (calculated in the range  $27^\circ \leq \theta \leq 145^\circ$ ), while it is 2.068 W for the twin jet, at an NPR value of 4.5. This represents an acoustic shielding effect of about 6%.

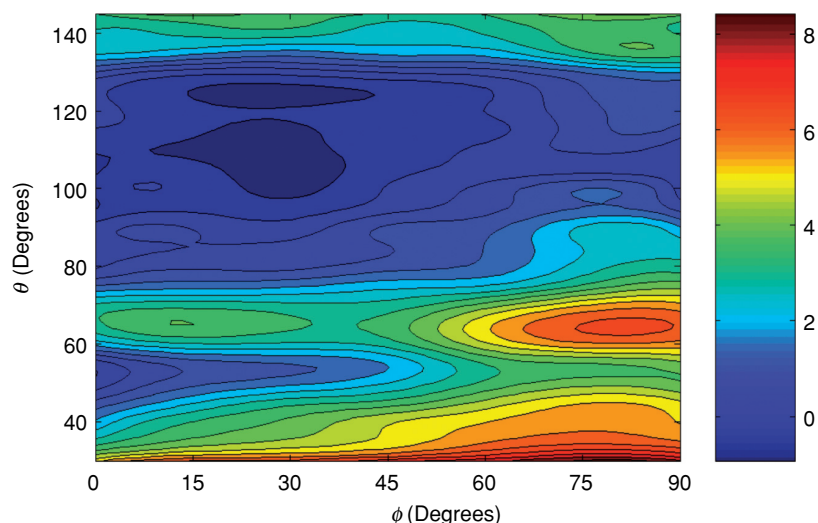


Figure 22: *Shielding contour map at NPR = 4.5 and  $s/h = 1.5$ .*

The noise reduction map at  $\text{NPR} = 4.5$  is shown in Fig. 22. This map is generated by plotting OASPL reduction (DOASPL) of twin jet (Vx-Vx) compared to single circular jet at various azimuthal and emission angles. In this color plot, dark blue corresponds to zero attenuation or slight amplification (0.5 dB), while other colors represent attenuation, with blue representing weak attenuations and red/brown indicating strong attenuations. It is clear that attenuation is higher in the downstream angles, while it is lower in the upstream angles, for almost all azimuthal angles. This clarifies the fact that basic directivity of sound sources in the jet plume overwhelms the azimuthal variations in the twin jet, as measured in the far field. However, the features of sharp variations in the azimuthal direction could emerge only from near field acoustic measurements.

#### 4. CONCLUSIONS

The screech tone is mostly inhibited in twin jets except for a few spacings and NPRs. Even though the screech tone is presented in Ed-Ed twin jet, the amplitude of the screech tone is 6 dB lower than the equivalent single (circular) jet screech tone. The 4 dB noise reduction in the twin jet OASPL compared to the equivalent single jet (circular and square) is due to fine scale turbulence structures from the sharp corners. The screech tone found in the non-interacting twin jets (Ed-Ed and Vx-Vx) at lower NPR is due to the presence of individual feedback loops in the twin jets. Though the screech tone is suppressed by increasing the jet spacing, the jet spacing is an ineffective tool to reduce the overall noise of the jet. The noise benefits of twin jets are significant at higher pressure ratios at all azimuthal angles. The twin jet becomes quieter than the addition of two single jets in the downstream angles. The acoustic shielding effect achieved by twin jets is around 6%. Thus, topological variations in initial conditions could serve as effective tools for noise suppression.

#### REFERENCES

- [1] E. J. Gutmark, F. F. Grinstein: Flow control with noncircular jets. *Annual Review of Fluid Mechanics* **31** (1999) 239-272.
- [2] W. R. Quinn, J. Militzer: Experimental and numerical study of a turbulent free square jet. *Physics of Fluids* **31** (1988) 1017-1025.

- [3] W. R. Quinn: Stream-wise Evolution of a square jet cross section. *AIAA Journal* **30** (1992) 2852-2857.
- [4] F. F. Grinstein, C. R. DeVore: Dynamics of coherent structures and transition to turbulence in free square jets. *Physics of Fluids* **8** (1996) 1237-1250.
- [5] K. Srinivasan, E. Rathakrishnan: Studies on polygonal slot jets. *AIAA Journal* **38** (2000) 1985-1987.
- [6] M. J. Lighthill: On sound generated aerodynamically. I. General theory. *Proc. Roy. Soc. London Ser.A* **211** (1952) 564-587.
- [7] A. Powell: On the noise emanating from a two-dimensional jet above the critical pressure. *Aeronautical Quarterly* **4** (1953) 103-122.
- [8] M. Harper-Bourne and M. J. Fisher: The noise from shock waves in supersonic jets. Noise mechanisms, AGARD CP **131** (1973), pp. 11-1-11-13.
- [9] J. M. Seiner, J. C. Manning, M. K. Ponton: Dynamic pressure loads associated with twin supersonic plume resonance. *AIAA Journal* **26** (1988) 954-960.
- [10] R. W. Wlezien: Nozzle Geometry Effects on Supersonic Jet Interaction. *AIAA Journal* **27** (1989) 1361-1367.
- [11] L. Shaw: Twin-jet screech suppression. *Journal of Aircraft* **27** (1990) 708-715.
- [12] G. Raman, R. Taghavi: Coupling of twin rectangular supersonic jets. *Journal of Fluid Mechanics* **354** (1998) 123-146.
- [13] G. Raman: Coupling of twin supersonic jets of complex geometry. *Journal of Aircraft* **36** (1999) 743-749.
- [14] W. V. Bhat: Experimental investigation of noise reduction from two parallel-flow jets. *AIAA Journal* **16** (1978) 1160-1167.
- [15] J. S. Clauss Jr., B. R. Wright, G. E. Bowie: Twin-jet shielding for a supersonic cruise vehicle. *Journal of Aircraft* **9** (1980) 627-632.
- [16] S. P. Parthasarathy, R. F. Cuffel, P. F. Massie: Twin-jet shielding. *Journal of Aircraft* **9** (1980) 618-626.
- [17] R. A. Kantola: Acoustic properties of heated twin jets. *Journal of Sound and Vibration* **79** (1981) 79-106.
- [18] B. N. Shivashankara, W. V. Bhat: Noise characteristics of two parallel jets with unequal flow. *AIAA Journal* **19** (1981) 442-448.
- [19] K. Srinivasan, S. Elangovan, E. Rathakrishnan: Twin elliptic jet as a candidate for attenuation of jet engine exhaust noise. *International Journal of Turbo and Jet Engines* **14** (1997) 99-104.
- [20] P. Panicker, K. Srinivasan, G. Raman: Aeroacoustic features of coupled twin jets with spanwise oblique shock-cells. *Journal of Sound and Vibration* **278** (2004) 155-179.
- [21] P. J. Morris, W. Richarz, H. S. Ribner: Reduction of peak jet noise using jet refraction. *Journal of Sound and Vibration* **29** (1973) 443-455.

- [22]C. H. Gerhold: Two dimensional analytical model of twin jet shielding. Journal of Acoustical Society of America **69** (1981) 904-908.
- [23]C. H. Gerhold: Analytical model of jet shielding. AIAA Journal **21** (1983) 694-698.
- [24]J. C. Yu, D. J. Fratello: Measurement of acoustical shielding by a turbulent jet. Journal of Sound and Vibration **98** (1985) 183-212.
- [25]T. W. Lancey: A quadrupole model for jet acoustical shielding. Journal of Sound and Vibration **179** (1995) 569-576.

#### **EARPHONES 'POTENTIALLY AS DANGEROUS AS NOISE FROM JET ENGINES'**

Turning the volume up too high on your headphones can damage the coating of nerve cells, leading to temporary deafness; scientists from the University of Leicester have shown for the first time. Earphones or headphones on personal music players can reach noise levels similar to those of jet engines, the researchers said. Noises louder than 110 decibels are known to cause hearing problems such as temporary deafness and tinnitus (ringing in the ears), but the University of Leicester study is the first time the underlying cell damage has been observed. The study has been published in the Proceedings of the National Academy of Sciences. University of Leicester researcher Dr Martine Hamann of the Department of Cell Physiology and Pharmacology, who led the study, said: "The research allows us to understand the pathway from exposure to loud noises to hearing loss. Dissecting the cellular mechanisms underlying this condition is likely to bring a very significant healthcare benefit to a wide population. The work will help prevention as well as progression into finding appropriate cures for hearing loss." Nerve cells that carry electrical signals from the ears to the brain have a coating called the myelin sheath, which helps the electrical signals travel along the cell. Exposure to loud noises – i.e. noise over 110 decibels – can strip the cells of this coating, disrupting the electrical signals. This means the nerves can no longer efficiently transmit information from the ears to the brain. However, the coating surrounding the nerve cells can reform, letting the cells function again as normal. This means hearing loss can be temporary, and full hearing can return, the researchers said. Dr Hamann explained: "We now understand why hearing loss can be reversible in certain cases. We showed that the sheath around the auditory nerve is lost in about half of the cells we looked at, a bit like stripping the electrical cable linking an amplifier to the loudspeaker. The effect is reversible and after three months, hearing has recovered and so has the sheath around the auditory nerve." The findings are part of ongoing research into the effects of loud noises on a part of the brain called the dorsal cochlear nucleus, the relay that carries signals from nerve cells in the ear to the parts of the brain that decode and make sense of sounds. The team has already shown that damage to cells in this area can cause tinnitus – the sensation of 'phantom sounds' such as buzzing or ringing.